

Transitions to turbulence in helium gas

F. Heslot, B. Castaing, and A. Libchaber

James Franck and Enrico Fermi Institutes, University of Chicago, 5640 S. Ellis Avenue, Chicago, Illinois 60637

(Received 13 July 1987)

Experimental study in gaseous helium at low temperature (4 K) of thermal convection up to a Rayleigh number $R=10^{11}$. Three regimes are observed, a chaotic state up to $R=2.5\times 10^5$, a soft-turbulence state up to $R=4\times 10^7$, and then a hard-turbulence state. We associate those three regimes to the boundary-layer formation and dynamics.

We present in this Rapid Communication preliminary results on a Rayleigh-Bénard experiment in gaseous helium at low temperature (4 K), and very high Rayleigh numbers (R). As shown by Threlfall¹ it is possible to cover 11 orders of magnitude in the Rayleigh number, with very small changes in the Prandtl number, by changing the pressure inside the cell.² Careful measurements of the Nusselt number (relative effective conductivity of the gas) led Threlfall to discover several transitions in the buoyancy state, as previously reported for other fluids by Malkus and others.³ In the experiment presented here, our main emphases are local measurements of the temperature at two different points inside the cell in order to characterize the various transitions. The main results are as follows. At low Rayleigh number we observe the onset of the oscillatory instability⁴ followed by the now well-known routes to chaos. We label the chaotic state itself in terms of the attractors correlation dimension. We then observe the transition to a spatial disorder through the loss of coherence between detectors for $R=2.5\times 10^5$. At higher Rayleigh numbers two successive regimes with slightly different power laws for the Nusselt number versus Rayleigh number are distinguished, the transition in our geometry being at $R=4\times 10^7$. The time recordings, power spectra, and histograms of the temperature fluctuations are different for the two regimes. We associate the two regimes to a laminar and a turbulent boundary layer.

A detailed description of the cell can be found and will be published.⁵ Let us give only its main spirit. The thin-wall stainless-steel cell is thermally isolated from the main liquid-helium bath by a vacuum jacket. It is a vertical cylinder with equal diameter and height (8.7 cm). The gas filling tube has a two-meter-long thermalization on the upper plate before entering the cell and can be closed near the cell in the helium bath. The upper plate is thermally regulated by a linear research LR-130 regulation system. The bottom plate is heated with a constant dc power, using a four-wire method for the precise measurement of power. Both plates are made out of thick electronic copper with calibrated Ge thermometers in each.⁶ Two local arsenic-doped silicon far-infrared detectors,⁷ 200 μm in size, are used to measure local temperature fluctuations. The "bottom" one is placed 200 μm above the bottom plate and inside the cell, and half a radius in distance from the cell axis. The "center" bolometer is placed right above the bottom one, at equal distances from both plates (see inset of Fig. 1).

Figure 1 shows the Nusselt number versus Rayleigh number dependence up to $R=10^{11}$. To span all this range we have used five different helium densities, whose corresponding pressures are 3, 8.5, 34, 138, and 625 Torr. This allowed large overlap in the study. The calibration between upper and lower thermometers was checked for each pressure, with corrections always inferior to 0.4 mK. We could thus be confident in results from temperature differences of $\Delta T \approx 3$ mK to $\Delta T \approx 1$ K, which represents more than two decades in R for each pressure. Four different domains in R number will be presented and are delineated in Fig. 1: The low R number including the chaotic state (R up to 2.5×10^5); the transition region where one loses coherence between bolometers (2.5×10^5 up to 5×10^5); a first turbulent state, which could be called "soft" turbulence and has many of the characteristics of large-aspect ratio-phase turbulence⁸ for R up to 4×10^7 ; finally, above this value a transition to a state showing large intermittency in the center bolometer, and the beginning of a power law for its spectrum. It could be associated with a turbulent boundary layer. We call it a "hard"-turbulence state.

In the first domain, the onset of convection ($R=5.8\times 10^3$ for this aspect ratio), the onset of the oscillatory instability (9×10^4), and the onset of a chaotic state (1.5×10^5) can be easily measured. Figure 2 shows typi-

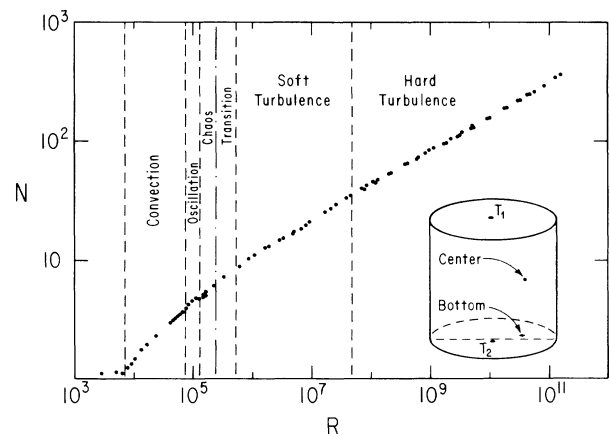


FIG. 1. Nusselt number vs Rayleigh number. The domains for the various transitions are defined. The inset shows a sketch of the experimental cell, whose height and diameter are 8.7 cm.

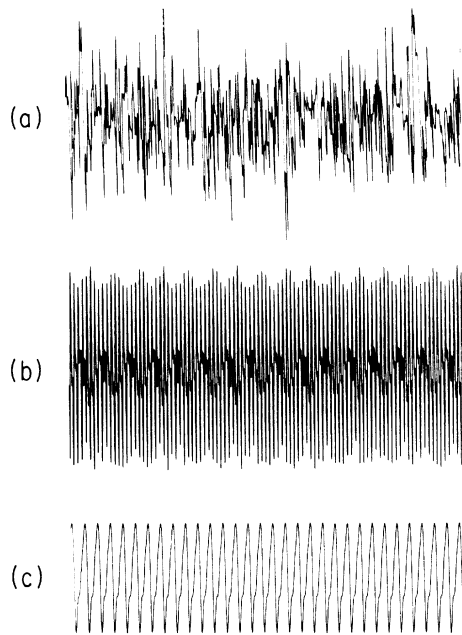


FIG. 2. Time recordings for three different states for the center bolometer. The time scales are different for each recording. (a) Soft turbulence, (b) quasiperiodicity, (c) oscillatory instability.

cal recordings of the local bolometers signal for the oscillatory region (c), and for a quasiperiodic state (b). In all this region, even in the chaotic state, the coherence function⁹ between the bottom and center bolometers is close to one for all significant frequencies. The routes to chaos observed included one through a period-doubling cascade, but this is by now well documented¹⁰ and we shall not detail it. Let us just remark that in this quite large cell, the signal to noise is above 80 dB, and thus with good stability and local bolometers, those routes to chaos can be studied in detail. We have measured the correlation¹¹ dimension D of the chaotic state. At the onset of chaos $D \approx 2 \pm 0.1$. It increases rapidly, reaching a value of $D=4$ at $R=2 \times 10^5$. As the number of points required to calculate the dimension increases exponentially with the dimension, the correlation dimension is a useful measure only for a relatively restricted range of Rayleigh numbers.

At $R=2.5 \times 10^5$ the coherence function between our two bolometers starts to decrease and at $R=5 \times 10^5$ it has a negligible value. This defines our second domain. The evolution is quite odd. First the amplitude of the coherence function decreases at low frequency but spreads to a higher frequency range before disappearing slowly. This transition region where the coherence between bolometers disappears, shows that the cell is now stratified with a different dynamical behavior near the center and close to the walls. We thus associate this transition with the formation of a boundary layer. Our main evidence for this is the Nusselt-number (N) evolution in the next domain, the third one, which goes up to $R=4 \times 10^7$.

The Nusselt-number evolution with R is well character-

ized there by the following curve-fitting formula

$$N = 1 + 0.096 \times R^{0.333 \pm 0.005} \quad (1)$$

The linear relation between N and $R^{1/3}$ is characteristic of a boundary-layer control flow,¹² indicating that the vertical length scale of the cell is no more relevant.

The power spectra of the two bolometers in this soft-turbulence regime are similar, with no power law. There are close to already published data⁸ on large aspect ratio cells, for low Rayleigh numbers. This suggests that we have a regime of detached boundary layers at the corners of the cell.¹³ Thus convective rolls germinate near the corners where an adverse pressure gradient is present, and this regime is similar to large-aspect ratio phase turbulence.^{8,14} A typical recording is shown in Fig. 2(a).

For $R=4 \times 10^7$ a transition to a new state, the fourth one in our nomenclature, occurs. Let us call it a hard-turbulence state. It is visible in the slope of the Nusselt number, which extends on four decades of Rayleigh numbers:

$$N = 1 + 0.2 \times R^{0.282 \pm 0.006} \quad (2)$$

Also, the shape of the temperature fluctuations in the center bolometer, its power spectrum, and histogram are different in this hard-turbulence state from the soft-turbulence one. The temperature recordings as a function of time for the two bolometers are shown in Fig. 3.

The histogram¹⁵ for the center probe, the probability density for the temperature fluctuations, is shown in Fig. 4. Its change of shape clearly reveals the transition. It is Gaussian-like for the soft-turbulence case [Fig. 4(a)] and exponential for the hard-turbulence one [Fig. 4(b)]. Also, the width of the distribution is smaller in the hard turbulence regime. This width decreases, as R increases, following a power law, but the shape remains the same for the highest R number studied.

We postulate that this is a regime of a turbulent boundary layer oscillating and with abrupt detachment of thermal plumes,¹² which leads to sharp temperature peaks

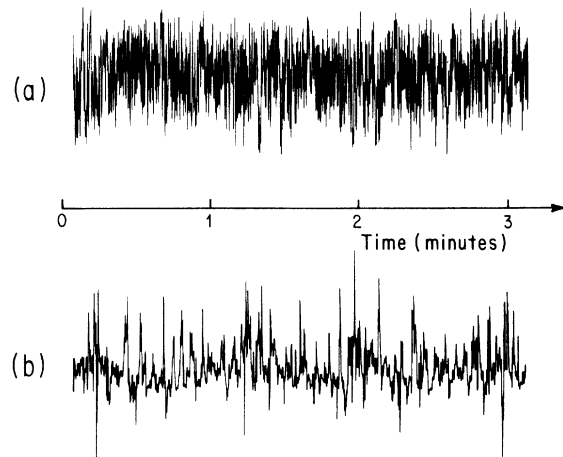


FIG. 3. Time recordings for the hard-turbulence state for $R=4 \times 10^9$. (a) Bottom bolometer, (b) center bolometer.

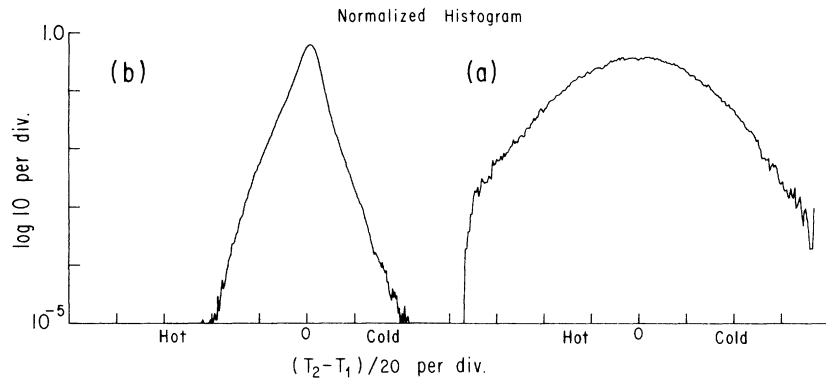


FIG. 4. Histogram of the time recordings: (a) soft-turbulence regime, (b) hard-turbulence regime. $T_2 - T_1$ represents the temperature difference across the cell.

in the center of the cell. Those plumes are localized objects, while in the soft turbulence, we have extended objects, the boundary between convective rolls.

The temperature recordings for the two bolometers is shown in Fig. 3. The center bolometer signal is characterized by a distribution of sharp peaks of variable heights. The bottom signal contains higher frequencies and also a well-defined oscillation at a frequency $1/t_0$, seen all over the cell, as can be measured from the coherence function shown in Fig. 5(c). This reemergence of coherence is one of the striking characteristics of the new state. Figures 5(a) and 5(b) show the Fourier spectra. One sees clearly that, above the frequency $1/t_0$, a power law develops for the center bolometer with a slope -1.4 ± 0.1 , and the power law tends to spread to a larger band of frequencies as the R number increases. Below $1/t_0$ the spectrum is flat.

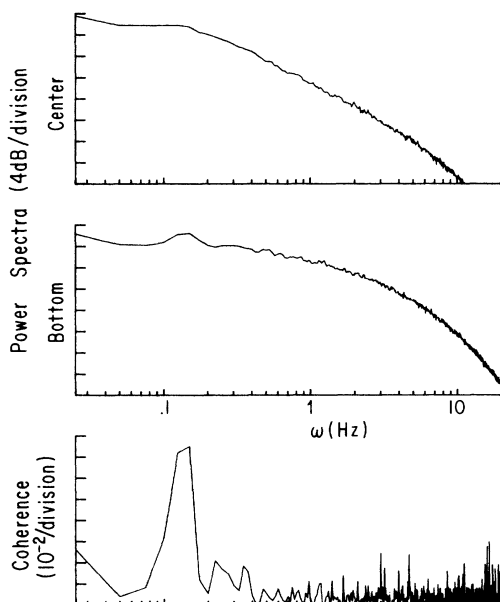


FIG. 5. Power spectra and coherence function for the center and bottom bolometer in the hard-turbulence state.

Looking at the distribution of the peaks in the center bolometer signal, we analyzed the time intervals between peaks, and found two groups in the density of time intervals. In the long-time group a well-developed peak also shows clearly the time t_0 . The short-time one could be characteristic of plumes, whereas t_0 seems to be the characteristic time of the convective circulation. We have measured the evolution of t_0 with R number and it follows:

$$1/t_0 = 5.10^{-2} R^{1/2} \text{ in units of } \kappa/L^2. \quad (3)$$

To sum up, the model proposed is that the distribution of peaks seen in the center bolometer, Fig. 3(b), is caused by thermal plumes emitted from the boundary layer. Through the stretching and folding of those detached plumes, by flow advection, the beginning of a developed turbulent state sets in.

In this experimental study of the transition from chaos to turbulence, we have in some ways brought together the two approaches of turbulence. The dynamical system approach¹⁰ is a very good analysis of the onset of disorder, as one slowly increases the R number starting from the onset of convection. It is followed by a state where space disorder sets in. In this regime, the development of a boundary layer,¹⁶ laminar first and later turbulent,¹⁷ leads to two distinct turbulent states, in agreement with a wealth of observations in fluid mechanics,¹⁸ and the description becomes more statistical in nature.¹⁹ One may suppose, but the experiments have to be performed, that at higher R numbers a fully developed turbulent state is present, but at what R number? By working near the critical point of helium we should be able to increase the control parameter by four orders of magnitude. The hard-turbulence state may be amenable to a statistical description. The soft-turbulence state might be more difficult to understand. We have thus outlined our program.

We would like to thank S. Thomae and L. Kadanoff for illuminating discussions. This work was supported by the National Science Foundation under Grant No. DMR-8316204.

¹D. C. Threlfall, Ph.D. thesis, University of Oxford, 1976 (unpublished); *J. Fluid Mech.* **67**, 1 (1975); **67**, 17 (1975). R. D. McCarthy, Nat. Bur. Stand. (U.S.) Tech. Note No. 631 (1972).

²We define the Rayleigh number as

$$R = g\alpha\Delta TL^3/\nu\kappa,$$

where g is the gravity acceleration, L is the height of the cell ($L=8.7$ cm), $\Delta T=T_2-T_1$, where T_2 is the bottom temperature and T_1 the top one. α is the isobaric thermal expansion, ν is the kinematic viscosity, and κ the heat diffusivity. These three quantities are taken at $T=(T_1+T_2)/2$.

³W. V. R. Malkus, *Proc. R. Soc. London Ser. A* **225**, 185 (1954); H. Janaka and H. Miyata, *Int. J. Heat Mass Transfer* **23**, 1973 (1980).

⁴F. H. Busse, *Rep. Prog. Phys.* **41**, 1928 (1978).

⁵F. Heslot, Thèse de Doctorat d'Etat, Université Paris VI, 1986 (unpublished).

⁶Cryocal, Germanium Thermometers GR1000.

⁷These bolometers are due to the courtesy of Professor R. Hildebrandt, Giles A. Novak, and M. Dragovan. See also, A. E. Lange, E. Kreysa, S. E. McBride, and P. L. Richards, *Int. J. Infrared Millimeter Waves* **4**, 689 (1983); J. C. Mather, *Appl. Opt.* **21**, 1125 (1982).

⁸G. Ahlers and R. P. Behringer, *Phys. Rev. Lett.* **40**, 712 (1978); A. Libchaber and J. Maurer, *J. Phys. (Paris) Lett.* **39**, 369 (1978).

⁹The coherence $C(w)$ between two signals is defined in the following way: Let $A(w)$ and $B(w)$ be their power spectra and

$K(w)$ the Fourier transform of their cross correlation. Then

$$C(w) = \frac{K(w)}{[A(w) \times B(w)]^{1/2}}.$$

¹⁰J. P. Eckmann, *Rev. Mod. Phys.* **53**, 643 (1981); *Universality in Chaos*, edited by P. Cvitanovic (Adam Hilger, Philadelphia, 1985).

¹¹P. Grassberger and I. Procaccia, *Physica D* **9**, 198 (1983); J. P. Eckmann and D. Ruelle, *Rev. Mod. Phys.* **57**, 617 (1985).

¹²L. M. Howard, in *Proceedings of the 11th International Congress of Applied Mechanics, Munich, 1964*, edited by H. Görtler (Springer, Berlin, 1964); D. J. Tritton, in *Turbulence and Predictability in Geophysical Fluid Dynamics and Climate Dynamics*, Proceedings of the Enrico Fermi School of Physics, Course 88, edited by M. Ghil, R. Benzi, and G. Parisi (North-Holland, Amsterdam, 1985).

¹³E. Reshotko, *Am. Rev. Fluid Mech.* **8**, 311 (1976).

¹⁴R. P. Behringer, *Rev. Mod. Phys.* **57**, 657 (1985); M. C. Cross and A. Newell, *Physica D* **10**, 299 (1984).

¹⁵We present, in fact, the probability density $P(T), P(T)dT$ being the probability for the bolometer to be found between the temperatures T and $T+dT$.

¹⁶T. J. Foster and S. Waller, *Phys. Fluids* **28**, 455 (1985).

¹⁷H. Schlichting, *Boundary Layer Theory* (McGraw-Hill, New York, 1979).

¹⁸D. J. Tritton, *Physical Fluid Dynamics* (Van Nostrand, New York, 1977), Chap. 11.

¹⁹H. Tennekes and J. L. Lumley, *A First Course in Turbulence* (MIT Press, Cambridge, MA, 1972).